

Hemodynamics of a Connecting conduit Between the Left Ventricle and the Left Descending Coronary Artery

Eun Bo Shim^{1¶}, and Jong Yub Sah²

¹ Department of Mechanical Engineering, Kangwon National University

² Department of Mechanical Engineering, Yeungnam University

Abstract

A new treatment for coronary artery occlusive disease is being developed in which a shunt or conduit is placed directly connecting the left ventricle with the diseased artery at a point distal to the obstruction. To aid in assessing and optimizing its benefit, a computational model of the cardiovascular system was developed and used to explore various design conditions. Simulation results indicate that in complete LAD occlusion, flow can be returned to approximately 65% of normal if the conduit resistance is equal for forward and reverse flow, increasing to 80% in the limit in which backflow resistance is infinite. Increases in flow rate produced by asymmetric flow resistance are considerably enhanced in the case of a partial LAD obstruction since the primary effect of resistance asymmetry is to prevent leakage back into the ventricle ("steal") during diastole. Increased arterial compliance has little effect on net flow with a symmetric shunt, but leads to considerable augmentation when the resistance is asymmetric. These results suggest that an LV-LAD conduit will be beneficial when stenosis resistance (R_{st}) > 27 PRU if resistance is symmetric.

Key words : Coronary Artery, Occlusion, LV-LAD Bybass, Lumped Parameter Model

Introduction

Current methods for treating coronary artery disease, either by coronary artery bypass (CABG) or coronary angioplasty, are generally successful and continue to be improved. Despite the excellent success of these methods, however, a significant number of patients experience repeated occlusion and ultimately reach a situation with few remaining

alternatives. The persistence of this patient subgroup in spite of the most recent advances in existing methods has motivated the search for entirely new treatment modalities including TMR(Transmyocardial revascularization)¹.

One recent approach now being investigated is to bypass the region of obstruction by means of a direct shunt between the left ventricle (LV) and the distal region of the obstructed vessel, here considered to be the left anterior descending (LAD) artery². Success of this approach is based on the hypothesis that the

¶ Hoja-dong, ChunChon, Kangwon-Do, 200-701, Korea
E-mail : ebshim@kangwon.ac.kr

forward flow generated during cardiac systole will outweigh the reverse flow, from the coronary arteries into the left ventricle, during diastole. Some success has been achieved with this method, though the conditions for optimal coronary artery perfusion remain unclear.

For normal case of coronary circulation, there have been many computational studies to explain the coronary hemodynamics. It is widely known that the computational approaches can be an effective mean to delineate coronary circulation in normal or pathological state. Beyar et al. provided the computational results of the transmural coronary flow patterns during normal and ischemic conditions are complex and relatively inaccessible to measurements^{3,4}. Schreiner et al. used a mathematical model to represent the vascular bed of the left coronary circulation by an arterial, a capillary and a venous compartment⁵. Epicardial coronary blood flow including the presence of stenoses and aorto-coronary bypasses has been delineated by Rooz et al⁶.

Due to the complexity of animal testing, and the natural variability experienced in biological experiments, there exists a need to develop rapid, systematic methods of analysis and optimization. Here we develop a computational model for the purpose of exploring different design conditions in the case of a LV-LAD conduit. Our purpose is to identify promising approaches that might then be further evaluated by experiments in test animals. We consider the dimensions of the connecting conduit, the benefits of producing asymmetric flow resistance through it, and the effects of variations in arterial compliance.

Methods

The proposed procedure introduces a direct connection between the left ventricle and a distal segment of the obstructed artery by insertion of a shunt between the left ventricle and the coronary artery directly through the myocardium (Figure 1). The shunt or conduit may be a simple tube of uniform internal diameter, or be shaped in such a way as to create conditions favoring flow into the arterial

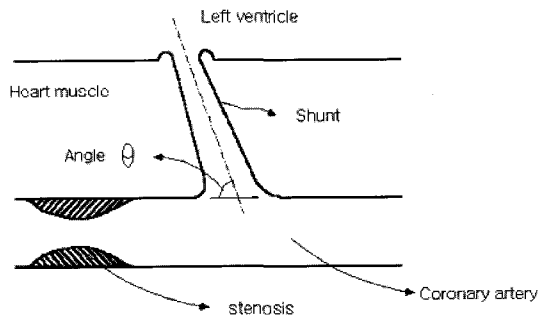


Figure 1 Schematic of the proposed surgical procedure.

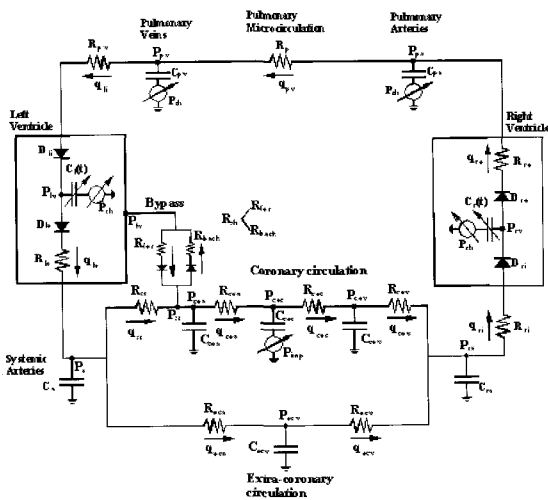


Figure 2 Schematic of a lumped parameter model of the total circulation emphasizing the coronary circulation.

segment rather than in the reverse direction as shown in the figure.

To investigate the hemodynamic effects of conduit insertion we implemented a computational code capable of simulating the dynamics of the cardiovascular system. Validation of the simulation was accomplished by comparison of model predictions with available experimental data.

In the present study, we modified an existing lumped parameter models of the entire cardiovascular (CV) system by adding a separate coronary circulation with greater detail (Figure 2)^{7,8}. Each compartment is characterized by an inflow resistance R expressed in peripheral resistance units (1 PRU = 1 mmHg·s/ml), a compliance or, in the electrical analogy, a capacitance C with units of ml/mmHg, a volume at zero transmural pressure V_0 (zero pressure

filling volume) with units of ml, and an outflow resistance. Transmural pressure across the pulmonary capacitance varies according to intrathoracic pressure. In order to simulate the effects of an LV-LAD shunt, the left ventricle is connected to the LAD by means of a pair of resistor-diode pairs, one to convey flow from the LV to the LAD ("forward" flow) and another to convey flow from the LAD into the LV ("reverse" flow). Diodes are introduced to ensure unidirectional flow through each pathway. Different resistance values can be assigned to each path to examine the potential benefit of a directional asymmetry in flow resistance. The model also simulates autoregulation as mediated by the baroreceptor reflex for short term control of blood pressure and the cardiopulmonary reflex for control of blood volume. These autoregulation capabilities are useful in examining a variety of realistic conditions that might be experienced by patients before and after conduit implantation. In addition, it provides the opportunity to study how the altered system will perform in conjunction with the rest of the circulation. It does not include local autoregulatory effects, however, as discussed further below.

Application of mass conservation and continuity of pressure at each node in the lumped parameter hemodynamic model leads to a matrix equation of the form:

$$dp/dt = Ap + b$$

Here p is the vector containing all compartmental pressures, A represents the time constants for exchange between compartments, and b is the input to the system. This initial value problem of ordinary differential equations is solved using a fourth order Runge-Kutta method yielding the pressures within each compartment and the flows between compartments, both as functions of time. A more detailed presentation of the model and the associated equations can be found in Appendix A for the coronary vessel network, and in Heldt et al. and Shim et al. for the systemic circulation^{7,8}. Values for each of

the model parameters and how they are selected, are discussed later and in Appendix B.

The reference value of conduit resistance is obtained by assuming Poiseuille flow (fully developed, steady and laminar). This should be viewed as a rough estimate of the actual flow resistance through the reference conduit since the effects of unsteadiness, flow separation, and small variations in internal geometry (among other factors) could exert a significant influence on this value. Flow rate, Q , through the conduit under this assumption is expressed as follows:

$$Q = \frac{A^2 \Delta P}{8\pi\mu L}$$

Here, A , ΔP , μ and L represent cross-sectional area, pressure drop, fluid viscosity, and conduit length respectively. From this relation we can estimate the resistance of the conduit:

$$R_{con} = \frac{\Delta P}{Q} = \frac{8\pi\mu L}{A^2}$$

Using typical values for the conduit diameter ($D=2$ mm) length ($L=2$ cm), and blood viscosity ($\mu=0.003$ kg/(m·s)), the resistance is calculated to be 1.147 PRU.

The conditions simulated correspond to an obstruction in the proximal left anterior descending (LAD) coronary artery, at a location approximately 2/3 the way down the vessel. Since normal values for LAD flow rate are in the range of 1 ml/s, we adjusted the coronary arteriolar resistance R_{coa} and coronary capillary resistance R_{coc} until baseline flow rate was 2/3 of the total LAD flow rate, or approximately 0.667 ml/sec in the absence of any constriction. The ratio of arteriolar to capillary resistance was taken to be 10 and assumed constant. Since our interest is in simulating cases of advanced disease, we assumed that the peripheral bed was maximally dilated, which we estimated to correspond to the case in which resistance was reduced to 20% of normal. Consequently, flow rate through the unobstructed vessel was 3.33 ml/s, five times as large as the assumed normal flow rate when there was no

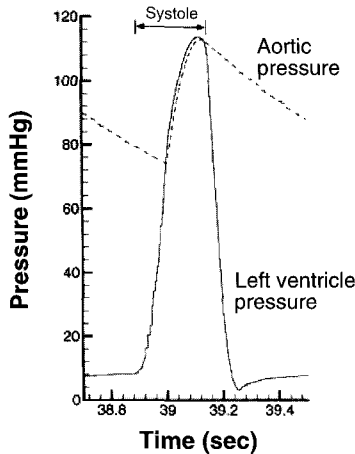


Figure 3 Computed left ventricular and aortic pressures.

proximal obstruction. Values of arteriolar and capillary resistance that produced this flow rate were $R_{coa}=13.5$ PRU and $R_{coc}=1.35$ PRU, respectively.

Results and Discussions

Since blood flow through the coronary circulation is small relative to that of the total circulation, the coronary circulation has little influence on the overall distribution of blood flow. Conversely, the aortic and left ventricular pressure determined from the overall circulation (Figure 3) is the main determinant of coronary blood flow.

For the purpose of verification we simulated the coronary circulation in a normal state and compared our results with the published results of Schreiner⁵. During systole, the coronary capillary flow rate decreases due to the increased resistance resulting from myocardial contraction, whereas flow through the coronary veins increases due to compression of the capillaries. Capillary and venous volumes vary in a manner similar to the flow rate variations shown in Figure 4, which is well compared with the result of Schreiner⁵.

For a fully occluded LAD, we compared our computational results with experimental measurements in a dog following placement of a conduit, done by Prof. Burkoff's group of Columbia university medical school². In these simulations, we varied the resistance of the stenosis R_{st} to simulate conditions ranging from total occlusion ($R_{st} = \infty$) to completely open and healthy ($R_{st} = 0$). For the case with total occlusion (Figure 6), computed results are

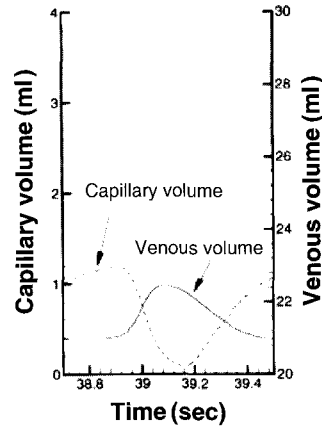


Figure 4 Computed coronary capillary and venous volume where systole period is from 38.89 to 39.14 sec.

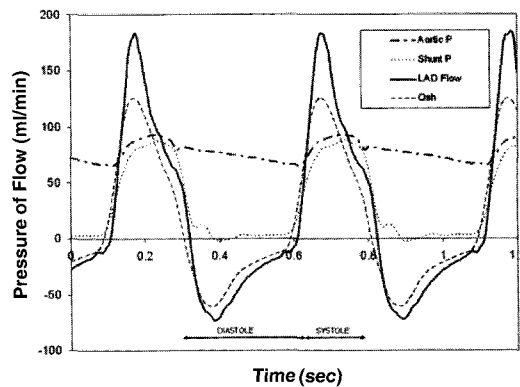


Figure 5 Time variations in critical hemodynamic variables with the coronary artery totally occluded (experiments on dogs).

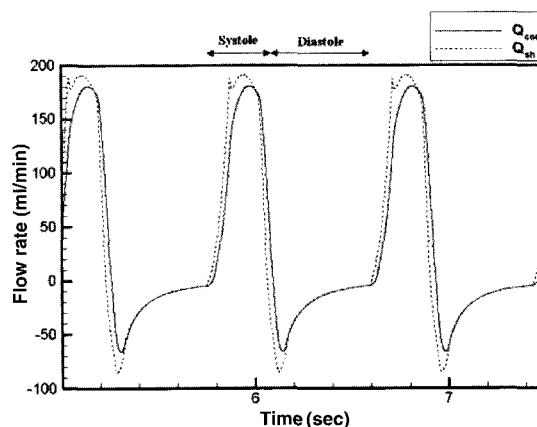


Figure 6 Computed flow rates of the LAD (Q_{coa}) and the shunt (Q_{sh}) with the proximal LAD totally occluded and the conduit in place.

similar to the available experimental measurements. Here, subscript 'sh' and 'coa' correspond to the conduit and coronary arterioles, respectively. Both

theory and experiment show a large peak in forward flow during systole and a smaller, but still significant negative flow during diastole, essential out-of phase with coronary artery flow in an unobstructed system.

An initial series of computations was performed to establish the relation between conduit resistance and flow rate through the conduit (Figure 7). In this case the LAD is fully occluded. According to the figure, the increase in conduit resistance induces a decrease

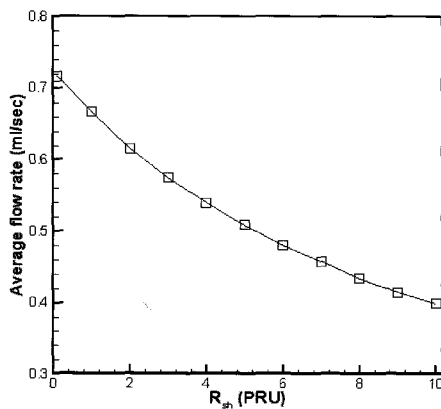


Figure 7 Variation of average LAD flow rate as a function of conduit resistance with the coronary artery totally occluded.

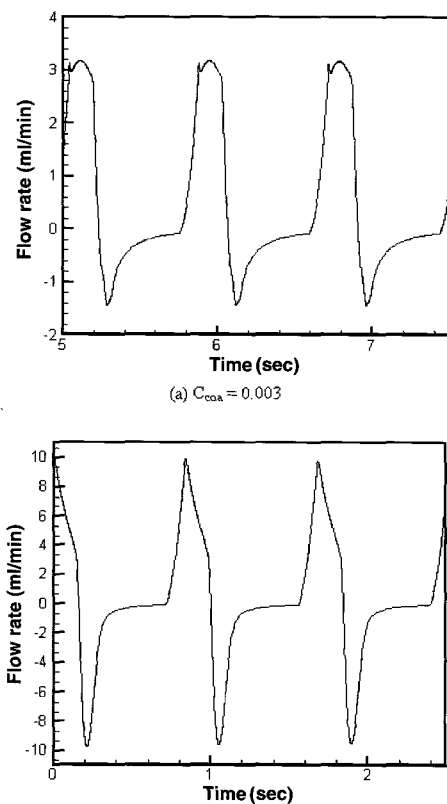


Figure 8 Time varying LAD flow patterns for two different values for arterial compliance.

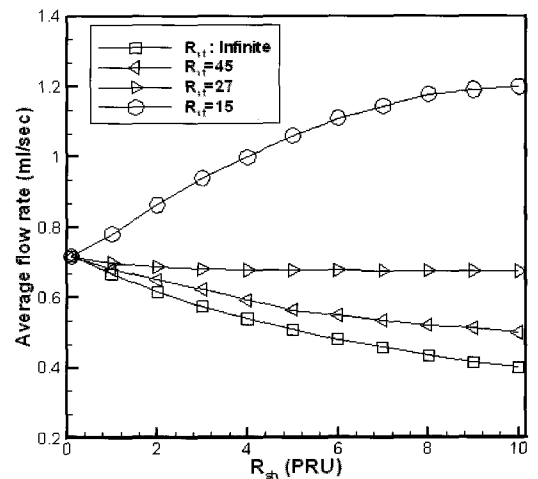


Figure 9 Average LAD flow rate according to the conduit resistance in several cases of stenotic resistance. Note that a resistance of 15 PRU represents about a 66% diameter reduction, 27 PRU about a 71% reduction, and 45 PRU a 74% reduction.

in the net flow rate through the conduit, as one would expect. Consequently, this plot indicates that minimal conduit resistance produces the greatest flow with LAD occlusion. It is also found that distal vessels must be maximally dilated for effective myocardial perfusion.

To test the effect of the compliance of the coronary artery we performed calculations for two values of compliance as represented in Figure 9: a normal value (0.003 ml/mmHg), and a higher value (0.03 ml/mmHg). The peak positive and negative flow rates with the higher epicardial capacitance are larger than that of the lower epicardial capacitance. However, the net (cycle-averaged) flow rate during one cardiac cycle is nearly identical in these two cases. Blood is simply shunted into and out of the arterial capacitance.

Since any blood that returns to the LV during diastole is essentially lost to the coronary circulation, it would seem advantageous to design a conduit tube that favors forward flow over reverse flow. As shown in Figure 1, the LV-LAD conduit might be tapered with a smaller diameter at the side of LV. This would produce a resistor with low forward (into the coronary artery) resistance and a higher reverse (out-of the coronary artery) resistance.

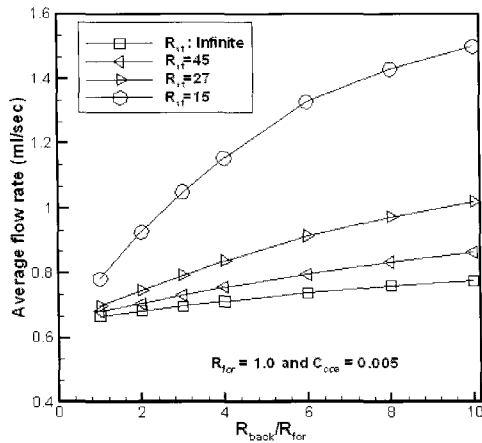


Figure 10 LAD flow rate as a function of the ratio of backward resistance to forward resistance, R_{back}/R_{for} .

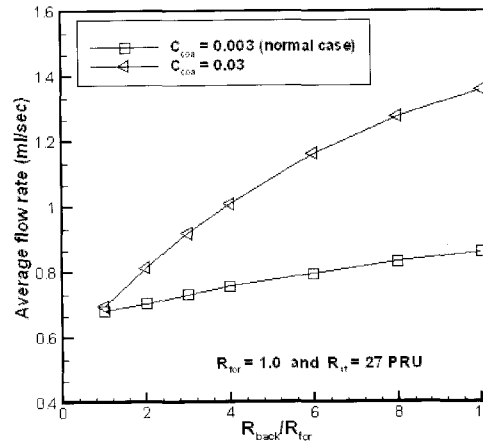


Figure 11 LAD flow rate as a function of the resistance ratio R_{back}/R_{for}

We have conducted parametric studies allowing to the ratio of backward resistance to forward resistance (the resistance ratio) to vary as presented in Figure 10. As in Figure 9, flow rate increases with a decrease in the stenosis resistance, going from one curve to the next. For any given stenosis severity, as the resistance ratio increases, the flow rate also goes up. However, the rate of increase slows as the ratio increases further. One interesting finding can be extracted from the combined results in Figure 9 and 10. In Figure 9, it is clear that if $R_{st} = 15$ PRU, the patient is better off without a LV-LAD conduit since the flow rate is greatest for R_{sh} approaching infinity. In Figure 10, however, it can be seen that this same patient benefits considerably from the placement of a conduit if the resistance ratio is large. For example, if $R_{back}/R_{for} = 10$, LAD flow rate is nearly 1.5 ml/s, much greater than the non-shunt flow of about 1 ml/s. It remains to be seen if a conduit with such large asymmetry can be produced.

To assess the effect of the compliance of the coronary artery in the case of an asymmetric resistance, a comparison is made between normal and high capacitance cases (Figure 11). Higher capacitance leads to somewhat greater flow rates at the same resistance ratio and the gradient of the increase in flow rate is much steeper than that of the normal capacitance.

Conclusions

In this study we provided the computational results of the hemodynamics of a connecting conduit between the left ventricle and the left descending coronary artery. To delineate the effect of the conduit, we implemented a computational code that can simulate the system dynamics of the cardiovascular system after insertion of the conduit. Many critical cases are predicted by this code and we compared these with available numerical and experimental data. The parametric studies of the simulation following the insertion surgery were conducted. Computational results showed that minimal shunt resistance produces the greatest flow with LAD occlusion. It was also found that distal vessels must be maximally dilated for effective myocardial perfusion. For a shunt with symmetric resistance, stenoses with a resistance of less than 27 PRU (<71% diameter reduction) do not benefit from shunt placement. In all situations with a symmetric resistance for which a shunt is beneficial, the greatest benefit is derived for the smallest resistance. We have conducted parametric studies allowing to the ratio of backward resistance to forward resistance to vary as presented. This computation indicates that flow rate increases with a decrease in the stenosis resistance, going from one curve to the next. For any given stenosis severity, as the resistance ratio increases, the flow rate also goes up. However, the rate of increase slows as the ratio increases further.

Appendix A: Detailed formulation of the coronary circulation analysis

In this section, we present the detailed expressions of the computational procedure to simulate coronary circulation. The schematic diagram of the computational code is represented in Figure 4.

Variables:

- P : Pressure (unit : mmHg)
- q : Flow rate (unit : ml/sec)
- R : Resistance (unit : mmHg sec/ml = PRU)
- C : Compliance (unit : ml/mmHg)
- D : Diode or check valve
- V : Volume (ml)

Subscripts:

- li : Left ventricle inflow
- lv : Left ventricle
- lo : Left ventricle outflow
- a : Systemic arteries
- st : Stenosis of coronary arteries
- by : Bypass connection from left ventricle
- sh : Conduit connection from left ventricle
- for : Conduit forward direction
- back : Conduit backward direction
- coa : Coronary arterioles
- coc : Coronary capillaries
- imp : Intra-myocardium
- cov : Coronary veins
- eca : Extracoronary arterioles
- ecv : Extracoronary veins
- ra : Right atrium
- ri : Right ventricle inflow
- rv : Right ventricle
- ro : Right ventricle outflow
- pa : Pulmonary arteries
- pv : Pulmonary veins
- th : Intrathoracic

The coronary circulation consists of three compartments: the coronary arteries, the coronary capillaries and the coronary veins. The effects of myocardial muscle contraction or relaxation is produced by temporal variations in the bias pressure $P_{imp}(t)$. The flow rates between the respective compartments are thus

$$q_{li} = \begin{cases} (P_{pv} - P_{lv}) / R_{pv} & \text{if } P_{pv} > P_{lv} \\ 0 & \text{otherwise} \end{cases} \quad (1)$$

$$q_{lo} = \begin{cases} (P_{lv} - P_a) / R_{lv} & \text{if } P_{lv} > P_a \\ 0 & \text{otherwise} \end{cases} \quad (2)$$

$$q_{st} = (P_a - P_{st}) / R_{st} \quad (3)$$

$$q_{sh} = (P_{lv} - P_{st}) / R_{sh} \quad \begin{cases} R_{sh} = R_{for} & \text{if } P_{lv} > P_{st} \\ R_{sh} = R_{back} & \text{if } P_{lv} < P_{st} \end{cases} \quad (4)$$

$$q_{coa} = \begin{cases} (P_{coa} - P_{coc}) / R_{coa} & \text{if } P_{coa} > P_{coc} \\ \frac{(P_{coa} - P_{coc})}{(R_{coa} + \beta / V_{coc}^2)} & \text{otherwise} \end{cases} \quad (5)$$

For the conduit resistance in Eq. 4, the resistance values of the conduit can be changed according to the direction of flow. The forward and backward resistances are shown in Figure 4. In Eq. 5, the flow rate to capillaries may be either forward (i.e. $q_{coa} > 0$) or retrograde, depending on the sign of the pressure gradient. However, reverse flow ceases as the capillary volume approaches zero since nothing then remains to be squeezed out. Moreover, as the capillary vessels are compressed, their resistance increases and they will throttle the flow. Accordingly, for a negative pressure gradient Eq. 5 reduces backward flow to zero as the capillary volume approaches zero. For flow into the veins and right atrium, a similar approach can be applied, producing the following two equations.

$$q_{coc} = \begin{cases} \frac{(P_{coc} - P_{cov})}{(R_{coc} + \beta / V_{coc}^2)} & \text{if } P_{coc} > P_{cov} \\ \frac{(P_{coc} - P_{cov})}{(R_{coc} + \beta / V_{cov}^2)} & \text{otherwise} \end{cases} \quad (6)$$

$$q_{cov} = \begin{cases} \frac{(P_{cov} - P_{ra})}{(R_{cov} + \beta / V_{cov}^2)} & \text{if } P_{cov} > P_{ra} \\ \frac{(P_{cov} - P_{ra})}{R_{cov}} & \text{otherwise} \end{cases} \quad (7)$$

$$q_{ecv} = (P_a - P_{ecv}) / R_{eca} \quad (8)$$

$$q_{ecv} = (P_{ecv} - P_{ra}) / R_{ecv} \quad (9)$$

$$q_{ri} = \begin{cases} (P_{ra} - P_{rv}) / R_{ri} & \text{if } P_{ra} > P_{rv} \\ 0 & \text{otherwise} \end{cases} \quad (10)$$

$$q_{ro} = \begin{cases} (P_{rv} - P_{pa}) / R_{ro} & \text{if } P_{rv} > P_{pa} \\ 0 & \text{otherwise} \end{cases} \quad (11)$$

$$q_{pv} = P_{pa} - P_{pv} / R_p \quad (12)$$

The state form of the node equations can be written in terms of these flow rates.

(a) Conservation of mass at the left ventricular node yields:

$$q_{ii} = q_{lo} + q'_{lv} \quad (13)$$

$$q'_{lv} = \frac{d}{dt} [C_l(P_{lv} - P_{th})] = C_l \frac{dP_{lv}}{dt} + (P_{lv} - P_{th}) \quad (14)$$

$$\therefore \frac{dP_{lv}}{dt} = \frac{q_{ii} - q_{lo} - (P_{lv} - P_{th}) dC_l(t)/dt}{C_l(t)} \quad (15)$$

(a) At the systemic arteries node :

$$q_{lo} = q_a + q'_a \quad (16)$$

$$q'_a = C_a \frac{dP_a}{dt} \quad (17)$$

$$\therefore \frac{dP_a}{dt} = \frac{q_{lo} - (q_{st} + q_{eca})}{C_a} \quad (18)$$

(b) At the coronary artery node :

$$q_a + q_{sh} = q_{coa} + q'_{coa} \quad (19)$$

$$q'_{coa} = C_{coa} \frac{dP_{coa}}{dt} \quad (20)$$

$$\therefore \frac{dP_{coa}}{dt} = \frac{(q_{st} + q_{sh}) - q_{coa}}{C_{coa}} \quad (21)$$

(c) At the coronary capillaries node :

$$q_{coa} = q_{coc} + q'_{coc} \quad (22)$$

where $q'_{coc} = C_{coc} \frac{d(P_{coc} - P_{imp})}{dt} \quad (23)$

$$\therefore \frac{dP_{coc}}{dt} = \frac{q_{coa} - q_{coc}}{C_{coc}} + \frac{dP_{imp}}{dt} \quad (24)$$

Capillary volume can be obtained by the relation.

$$V_{coc} = C_{coc} (P_{coc} - P_{imp}) \quad (25)$$

(d) Mass conservation at the coronary veins node :

$$q_{coc} = q_{cov} + q'_{cov} \quad (26)$$

where $q'_{cov} = C_{cov} \frac{dP_{cov}}{dt} \quad (27)$

$$\therefore \frac{dP_{cov}}{dt} = \frac{q_{coc} - q_{cov}}{C_{cov}} \quad (28)$$

For the capillary veins, venous pressure is calculated from the pressure-volume relation:

$$P_{cov} = V_{cov}^0 C_{cov}^0 e^{\sigma(V_{cov} - V_{cov}^0)} \quad (29)$$

corresponding to a volume-dependent compliance, defined as the derivative of V_{cov} with respect to P_{cov} :

$$C_{cov}(V_{cov}) = \frac{dV_{cov}}{dP_{cov}} = C_{cov}^0 (1 + \sigma V_{cov})^{-1} e^{-\sigma(V_{cov} - V_{cov}^0)} \quad (30)$$

Here, V_{cov}^0 , C_{cov}^0 are the reference venous volume and compliance, respectively, and σ is the slope of the change in compliance.

(e) Mass conservation at the extra-coronary veins node :

$$q_{eca} = q_{ecv} + q'_{ecv} \quad (31)$$

where $q'_{ecv} = C_{ecv} \frac{dP_{ecv}}{dt} \quad (32)$

$$\therefore \frac{dP_{ecv}}{dt} = \frac{q_{eca} - q_{ecv}}{C_{ecv}} \quad (33)$$

(f) At the right atrium node :

$$q_{cov} + q_{ecv} = q_{ri} + q'_{ra} \quad (34)$$

where $q'_{ra} = C_{ra} \frac{dP_{ra}}{dt} \quad (35)$

$$\therefore \frac{dP_{ra}}{dt} = \frac{q_{cov} + q_{ecv} - q_{ri}}{C_{ra}} \quad (36)$$

(g) At the right ventricle node :

By the same procedure with Eq. 15, we can get the equation for the right ventricle node.

$$\frac{dP_{rv}}{dt} = \frac{q_{ri} - q_{ro} - (P_{rv} - P_{th}) dC_r(t)/dt}{C_r(t)} \quad (37)$$

(h) At the pulmonary arteries node :

$$\frac{dP_{pa}}{dt} = \frac{q_{ro} - q_{pv}}{C_{pa}} \quad (38)$$

(i) At the pulmonary veins node :

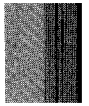
$$\frac{dP_{pv}}{dt} = \frac{q_{pv} - q_{ii}}{C_{pv}} \quad (39)$$

Appendix B: Parameter Values

Compartment	R _{in} (PRU)	R _{out} (PRU)	C (ml/mmHg)	V ₀ (ml)	Sources
Left heart	0.01 (R _{pv})	0.006 (R _{lo})	0.4 ~ 10	15	Suga et al., 1974 ⁹ ,
Systemic arteries	0.006 (R _{ca})	0.05 (R _a)	1.6	715	Beneken et al., 1967 ¹⁰
Extra-coronary	1.00 (R _{ea})	13.5 (R _{coa})	90	2450	Ursino, 1998 ¹¹
Veins	(variable)	1.37 (R _{co})	0.4	0.0	Sato et al., 1974 ¹²
Coronary arteries	13.5 (R _{coa})	0.6 (R _{cov})	0.25 (Variable)	25	Schreiner, 1990 ⁵
Coronary capillaries	1.37 (R _{co})	0.0025 (R _a)	31.0	25	Schreiner, 1990 ⁵
Coronary veins		0.003 (R _{ro})	1.2 ~ 20	15	Schreiner, 1990 ⁵
Right atrium		0.08 (R _{rp})	4.3	90	Ursino, 1998 ¹¹
Right heart	0.0025 (R _a)	0.01 (R _{pv})	8.4	490	Dell'Italia et al., 1988 ¹³
Pulmonary arteries	0.003 (R _{ro})				Beneken et al., 1967 ¹⁰
Pulmonary veins	0.08 (R _{rp})				Milnor, 1972 ¹⁴
Stenosis	Resistance : Variable				
Bypass resistance	R _{by} = 0.0001				
Intramyocardium Pressure	P _{imp} (t) = 0.75xP _{LV} (t)				
Total blood volume	V _{tot} = 5000 ml				
Reference coronary venous volume	V _{cov} ⁰ = 25 ml				
Reference coronary venous volume	C _{cov} ⁰ = 0.25 ml/mmHg				

References

1. Frazier OH. March RJ. Horvath KA. Transmyocardial Revascularization With A Carbon Dioxide Laser In Patients With End-Stage Coronary Artery Disease, New England Journal of Medicine 1999;341:1021-1028.
2. Suehiro K. Shimizu J. Yi GH. Zhu SM. Gu A. Sciacca RR. Wang J. and Burkhoff D. Direct coronary artery perfusion from the left ventricle. J Thorac Cardiovasc Surg. 2001;121:307-315.
3. Beyar R. Guerci AD. Halperin HR. Tsitlik JE. Weisfeldt ML. Intermittent coronary sinus occlusion after coronary arterial ligation results in venous retroperfusion. Circ Res. 1989;65(3):695-707.
4. Beyar R. Caminker R. Manor D. Sideman S. Coronary flow patterns in normal and ischemic hearts: transmyocardial and artery to vein distribution. Ann Biomed Eng. 1993;21(4):435-58.
5. Schreiner W. Neumann F. Mohl W. Coronary perfusion pressure and inflow resistance have different influence on intramyocardial flows during coronary sinus interventions. Med Phys 1990;17(6):1023-31.
6. Rooz E. Wiesner TF. and Nerem RM. Epicardial coronary blood flow including the presence of stenoses and aorto-coronary bypasses-I: Model and numerical method. J Biomech Eng. 1985;107(4): 361-367.
7. Heldt T. Shim EB. Kamm RD. Mark RG. Computational modeling of cardiovascular response to orthostatic stress. J Appl Physiol. 2002;92(3):1239-1254.
8. Shim EB. Youn CH. Heldt T. Kamm RD. and Mark RG. Computational Modeling of the Cardiovascular System After Fontan Procedure. Lecture Notes in Computer Science 2002;2526:105~114.
9. Suga H. and Sagawa K. Models of circulatory



- mechanics. *Circulation Research*. 1982;35:117.
10. Beneken JEW. and B. DeWitt. A Physical Approach to Hemodynamic Aspects of the Human Cardiovascular System. in *Physical Bases of Circulatory Transport: Regulation and Exchange*, E.B.a.G. Reeve, A.C., Editor. W.B. Saunders: Philadelphia 1967:1~45.
11. Ursino M. Interaction between carotid baroregulation and the pulsating heart: a mathematical model. *Am., J. Physiol.* 1998; 275: H1733-H1747.
12. Sato K. Yamamoto S. Vega D. and Grodins F. Parameter sensitivity analysis of a network model of systemic circulatory mechanics. *Annals of Biomedical Engineering* 1974;2:289-306.
13. Dell'Italia LJ. and RA. Walsh. Application of a time varying elastance model of right ventricular performance in man. *Cardiovascular Research* 1988; 22: 864-874.
14. Milnor WR. Pulmonary hemodynamics, in *Cardiovascular Fluid Dynamics*. D.H. Bergel, Editor, Academic Press: London 1972; 299-340.